Vectorial proteomics reveal targeting, phosphorylation and specific fragmentation of polymerase I and transcript release factor (PTRF) at the surface of caveolae in human adipocytes

Nabila ABOULAICH, Julia P. VAINONEN, Peter STRÅLFORS[1] and Alexander V. VENER[1]

Division of Cell Biology and Diabetes Research Centre, Faculty of Health Sciences, Linköping University, SE58185 Linköping, Sweden

Caveolae, the specialized invaginations of plasma membranes, formed sealed vesicles with outwards-orientated cytosolic surface after isolation from primary human adipocytes. This morphology allowed differential, vectorial identification of proteins at the opposite membrane surfaces by proteolysis and MS. Extracellular-exposed caveolae-specific proteins CD36 and copper-containing amine oxidase were concealed inside the vesicles and resisted trypsin treatment. The cytosol-orientated caveolins were efficiently digested by trypsin, producing peptides amenable to direct MS sequencing. Isolation of peripheral proteins associated with the cytosolic surface of caveolae revealed a set of proteins that contained nuclear localization signals, leucine-zipper domains and PEST (amino acid sequence enriched in proline, glutamic acid, serine and threonine) domains implicated in regulation by proteolysis. In particular, PTRF (polymerase I and transcript release factor) was found as a major caveolae-associated protein and its co-localization with caveolin was confirmed by immunofluorescence confocal microscopy. PTRF was present at the surface of caveolae in the intact form and in five different truncated forms. Peptides (44 and 45 amino acids long) comprising both the PEST domains were sequenced by nanospray-quadrupole-time-of-flight MS from the full-length PTRF, but were not found in the truncated forms of the protein. Two endogenous cleavage sites corresponding to calpain specificity were identified in PTRF; one of them was in a PEST domain. Both cleavage sites were flanked by mono- or diphosphorylated sequences. The phosphorylation sites were localized to Ser-36, Ser-40, Ser-365 and Ser-366 in PTRF. Caveolae of human adipocytes are proposed to function in targeting, relocation and proteolytic control of PTRF and other PEST-domain-containing signalling proteins.

Key words: caveolae, human adipocyte, MS, PEST sequence, polymerase I and transcript release factor (PTRF), proteolysis.

INTRODUCTION

Caveolae, flask-shaped invaginations in the plasma membrane, are found in many cells and particularly abundant in endothelial cells and adipocytes [1–3]. Caveolae are crucially involved in the uptake and transport of different molecules via endocytosis, transcytosis or potocytosis and are also involved in cholesterol homoeostasis [1]. In addition to being dynamic elements representing vesicular trafficking of substances into the cell, caveolae facilitate and integrate cell-surface-receptor-initiated signalling by concentrating different proteins and signalling molecules [4–6]. Specifically, in fat cells, the insulin receptor is localized in caveolae [7]. It has been suggested that caveolae are formed from lipid rafts in the membrane. Both rafts and caveolae are enriched in and structurally dependent on cholesterol and sphingomyelin [1,8]. A difference between the flat rafts and the flask-like caveolae membrane domains is determined by the protein caveolin, which appears to be crucial for the formation and structure of caveolae [9,10]. Caveolin is an integral membrane protein with N- and C-termini both exposed at the cytosolic surface of the plasma membrane [10]. The N-terminal domain of caveolin can interact with and concentrate, at the caveolae surface, a number of signal transduction proteins, such as G-proteins, Src-like kinases, protein kinase C and H-Ras [1]. The distinct assembly of proteins associated with caveolae may determine their specific functions in different cells and physiological conditions [2].

The typical morphology of caveolae and the presence of caveolin has formed the basis for using electron microscopy and immunogold labelling to study the presence of specific proteins in caveolae [7,11,12]. Different methods have also been used to isolate caveolae for identifying their protein content. These methods have utilized the presence of caveolin and the buoyancy of caveolae membranes in density-gradient centrifugation [12,13]. A study of immunopurified caveolae from rat adipocytes has demonstrated their limited protein composition [14]. On the contrary, proteomic studies of lipid rafts and caveolae prepared as detergent-resistant membranes of whole cultured Jurkat T cells [15,16] and human endothelial cells [17] have revealed a significant amount of signalling proteins associated with these membrane domains. An innovative approach for unbiased proteomics of lipid rafts [18] has yielded 241 proteins outlined as ‘authentic lipid raft components’. These proteins were dependent on cholesterol for associating with detergent-resistant or alkali-sonicated membranes of whole HeLa cells [18].

In the present study, we present vectorial proteomics as an approach for the characterization of caveolae isolated from physiologically relevant primary human adipocytes. Using the intrinsic property of caveolae to form vesicles with outwards-orientated cytosolic surface, we apply proteolytic digestion and MS for the differential localization and identification of protein domains exposed to the opposite surfaces of the caveolae membrane. We identify the most abundant proteins associated with the

Abbreviations used: CID, collision-induced dissociation; EHD, Eps15 homology domain; EHD2, EHD-containing protein 2; ESI, electrospray ionization; IMAC, immobilized metal affinity chromatography; MALDI–TOF-MS, matrix-assisted laser-desorption ionization–time-of-flight mass spectrometry; PTRF, polymerase I and transcript release factor; SDPR, serum deprivation response gene product; SRBC, serum deprivation response-related gene product that binds to C-kinase.

[1] Correspondence may be addressed to either author (email aleve@ibk.liu.se and peter.stralfors@ibk.liu.se).

cytoplasmic surface of the vesicles. Five of these proteins, including a regulator of transcription, PTRF (polymerase I and transcript release factor), contain PEST (amino acid sequence enriched in proline, glutamic acid, serine and threonine) domains; PEST domains are known to serve as recognition domains for regulating signalling proteins by proteolysis [19]. In the present study, we establish that most of the cellular PTRF is confined to plasma membranes and the protein is concentrated in caveolae. In addition, we found apparently *in vivo*-originated fragments of PTRF at the caveolae surface. We identified two endogenous cleavage sites in PTRF, one of which is in a PEST domain. Both cleavage sites are flanked by mono-serine-phosphorylated or doubly serine-phosphorylated sequences. Our findings suggest that caveolae in human adipocytes are involved in the binding, relocation and phosphorylation-related proteolytic control of the transcription regulator PTRF and probably also of other PEST-domain-containing signalling proteins found at the caveolae surface.

EXPERIMENTAL

Isolation of human adipocytes and preparation of caveolae and subcellular fractions

Fat tissue was obtained during elective abdominal surgery on female patients. The Local Ethics Committee approved our study and all participants gave their informed approval. Adipocytes were isolated by collagenase digestion of subcutaneous human fat tissue and homogenized as described in [7]. Homogenization was at room temperature (22 °C) in 10 mM NaH_2PO_4 (pH 7.4), 1 mM EDTA, 0.25 M sucrose, 25 mM NaF, 1 mM Na_4-PP_i, 2 mM Na_3VO_4, 0.5 mM EGTA, 4 mM iodoacetate, 10 μM leupeptin, 1 μM pepstatin, 1 μM aprotinin and 100 μM PMSF. A plasma-membrane-containing pellet obtained by centrifugation at 16 000 ***g*** for 20 min was resuspended in 10 mM Tris/HCl, 1 mM EDTA and 2 mM Na_3VO_4 with or without the protease inhibitors listed above. Plasma-membrane and mitochondrial/nuclear fractions were then separated by sucrose density-gradient centrifugation [20]. Nuclei were also prepared from the adipocytes in separate isolations, as described in [21]. A supernatant obtained after centrifugation at 16 000 ***g*** (see above) was further centrifuged at 200 000 ***g*** for 75 min to separate the microsomal and cytosol fractions. The pellet containing the microsomal fraction was resuspended in 50 mM NH_4HCO_3 (pH 8).

Caveolae membranes were prepared from the purified plasma membrane by sonication in 0.5 M Na_2CO_3 (pH 11) [13] and ultracentrifugal floatation as described in [7]. To isolate caveolae vesicles with associated non-integral membrane proteins, the purified plasma-membrane fraction was resuspended and sonicated in 50 mM NH_4HCO_3 (pH 8). The homogenate was adjusted to 45 % sucrose in 12 mM Mes (pH 6.5) and 75 mM NaCl and placed at the bottom of an ultracentrifuge tube containing 5–35 % discontinuous sucrose gradient in 12 mM Mes/50 mM NH_4HCO_3. A light-scattering band (caveolae-enriched fraction) at the 5–35 % sucrose interface obtained by centrifugation at 250 000 ***g*** for 16–20 h in an SW41 rotor (Beckman Instruments) was collected. Caveolae were then resuspended in 0.5 M $(NH_4)_2CO_3$ and adjusted to pH 11 by NH_4OH. The proteins released from the surface of caveolae vesicles (caveolae-associated proteins) were separated from membrane proteins by centrifugation at 170 000 ***g*** for 1 h. All steps were performed at 4 °C, and protease inhibitors, described above, were either included in or excluded from the homogenization and all subsequent steps, as indicated.

Trypsin treatment of membrane vesicles and caveolae-associated proteins

Isolated caveolae were washed three times with 25 mM NH_4HCO_3 (pH 8) and adjusted to a final protein concentration of 3 mg/ml. To remove the high concentration of $(NH_4)_2CO_3$ from caveolae-associated proteins, they were freeze-dried in a vacuum centrifuge five times with successive additions of deionized water before each freeze-drying. The proteins were finally resuspended in 25 mM NH_4HCO_3. Both caveolae and caveolae-associated proteins were reduced with 2 mM dithiothreitol, alkylated with 6 mM iodoacetamide and digested with trypsin (sequence-grade modified trypsin; 1 μg per 50 μg of sample protein for 24 h at 37 °C; Promega). The peptides released by trypsin from the caveolae were collected in the supernatant after centrifugation at 170 000 ***g*** for 20 min.

Enrichment of phosphopeptides by IMAC (immobilized metal affinity chromatography)

Peptides from caveolae-associated proteins were methyl-esterified by 2 M methanolic HCl, and phosphorylated peptides were enriched by IMAC as described in [22]. The IMAC procedure was modified as follows. The microcolumns containing 7 μl of chelating Sepharose (Amersham Biosciences, Uppsala, Sweden) were prepared in GELoader tips (Eppendorf, Hamburg, Germany) and loaded with 100 μl of 0.1 M $FeCl_3$. Unbound Fe ions were removed by washing with 40 μl of 0.1 % (v/v) acetic acid. The mixture of methylated caveolae peptides in 10 μl of methanol/water/acetonitrile (1:1:1, by vol.) was loaded on to the column, which was washed with 2 × 20 μl of 0.1 % acetic acid in water, 2 × 20 μl of 0.1 % acetic acid in 20 % (v/v) acetonitrile and 2 × 20 μl of 20 % acetonitrile in water. Phosphopeptides were eluted by four washings with 10 μl of 20 mM Na_2HPO_4 in 20 % acetonitrile. The four eluted fractions were collected separately and desalted using a C_{18} ZipTip (Millipore, Bedford, MA, U.S.A.).

SDS/PAGE and immunoblotting

Subcellular fraction and caveolae proteins were separated by SDS/PAGE (9 % gel). The separated proteins were stained with Coomassie Blue or silver. For immunoblotting, the proteins were transferred on to PVDF membranes (Millipore). The membranes were then blocked with milk proteins or BSA, incubated with rabbit anti-caveolin-1 polyclonal antibody, rabbit anti-insulin receptor β-subunit polyclonal antibody, mouse anti-nucleoporin-p62 monoclonal antibody, mouse anti-phosphotyrosine PY20 monoclonal antibody (Transduction Laboratories, Lexington, KY, U.S.A.) or mouse anti-PTRF monoclonal antibody (BD Biosciences, San Diego, CA, U.S.A.) as indicated, followed by ECL® according to the manufacturer's instructions (Amersham Biosciences, Little Chalfont, Bucks., U.K.) and evaluated by chemiluminescence imaging (Las 1000; Fuji, Tokyo, Japan).

Immunofluorescence microscopy of plasma-membrane sheets

Plasma-membrane sheets were prepared as described by Thorn et al. [3]. Briefly, the adipocytes were rinsed in ice-cold phosphate buffer (10 mM Na_2HPO_4, 1.8 mM KH_2PO_4 and 150 mM NaCl, pH 7.5) and then attached to poly-L-lysine-coated coverslips. Coverslips with the captured adipocytes were flushed with ice-cold 150 mM KCl and 1.9 mM Tris/HCl buffer (pH 7.5). The plasma membranes remaining on the coverslips were rinsed three times in 150 mM Hepes (pH 7.5) and fixed for 30 min in phosphate buffer supplemented with 3 % (w/v) paraformaldehyde.

After treatment with 0.1 % $NaBH_4$ for 15 min, the membranes were blocked with phosphate buffer containing 5 % (v/v) BSA for 60 min at 37 °C. Then, coverslips were incubated with the indicated primary antibodies for 90 min at 37 °C and rinsed with 0.1 % BSA in phosphate buffer (pH 7.5). Finally, coverslips were incubated with secondary fluorescent Alexa antibodies (Molecular Probes, Leiden, The Netherlands), which were subsequently detected with a Nikon eclipse D1 confocal microscope (Tokyo, Japan).

MALDI–TOF-MS (matrix-assisted laser-desorption ionization–time-of-flight mass spectrometry)

For in-gel digestion, protein bands were excised from the gel slab and treated with trypsin (sequencing-grade modified trypsin; Promega) essentially as described in [23]. Tryptic peptides were analysed by MALDI–TOF-MS using a Voyager-DE™ Pro (Applied Biosystems, Framingham, MA, U.S.A.). For peptide mass 'fingerprint' analysis, equal volumes of the sample and α-cyano-4-hydroxycinnamic acid in 70 % acetonitrile with 0.3 % (v/v) trifluoroacetic acid were spotted on the target plate. The acceleration voltage was 20 kV, grid voltage 75 %, guide wire 0.02 and the extraction delay time 200 ns. Reflector mass spectra were acquired and calibrated either externally or internally, using trypsin autolysis peptides.

ESI (electrospray ionization) tandem MS

The experiments were performed on a hybrid mass spectrometer, API Q-STAR *Pulsar i* (Applied Biosystems, Foster City, CA, U.S.A.) equipped with a nanoelectrospray ion source (MDS Protana, Odense, Denmark). Samples were desalted on a C_{18} reversed-phase Zip Tip according to the manufacturer's instructions (Millipore) and 2 μl of eluted peptide solutions (50 % acetonitrile in water with 1 % formic acid) were then loaded on to the nanoelectrospray capillaries. Mass spectra and spectra of peptide fragments after CID (collision-induced dissociation) of selected peptide ions were acquired with instrument settings recommended by Applied Biosystems.

RESULTS

Isolation of caveolae

We isolated caveolae from purified plasma membranes of human adipocytes using a detergent-free procedure [7,13]. The pattern of the proteins in isolated plasma membranes, caveolae and mitochondrial/nuclear membranes is shown in Figure 1(A). The protein patterns in caveolae and plasma membranes were rather similar, in agreement with an earlier finding that caveolae constitute a substantial part of the plasma membrane in adipocytes [3]. Immunoblot analyses with antibodies against caveolin and the insulin receptor (Figure 1B) confirmed significant enrichment of these two proteins in the isolated caveolae. To verify that caveolae were not contaminated with mitochondrial/nuclear membranes, seven protein bands, characteristic of the latter fraction (numbered in Figure 1A), were excised from the gel, digested with trypsin and analysed by peptide mass 'fingerprinting' and peptide sequencing using ESI–MS and CID. The same analyses were performed on the corresponding gel slices from the caveolae fraction. Table 1 summarizes the results, which identified nine mitochondrial proteins. Notably, none of these nine proteins was found in the caveolae fraction, which confirmed the absence of mitochondrial contamination in the isolated caveolae. The mitochondrial/nuclear fraction (Figure 1A) was composed mostly of mitochondrial

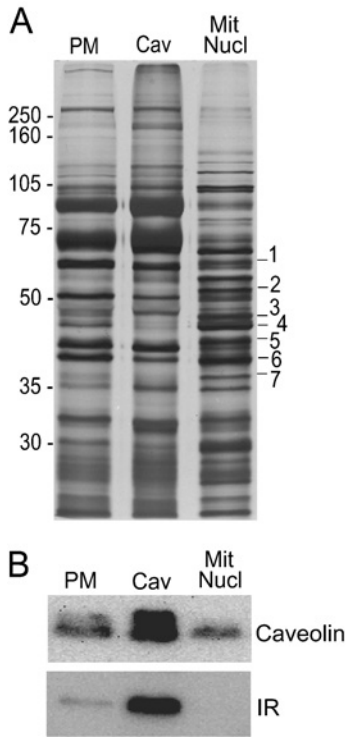

Figure 1 Characterization of caveolae purity

(**A**) Protein patterns in plasma-membrane (PM), caveolae (Cav) and mitochondrial/nuclear (Mit/Nucl) fractions revealed by SDS/PAGE and silver staining (5 μg of protein was loaded in each lane). Molecular-mass standards (kDa) are indicated. The protein band numbers on the right correspond to the numbers of identified proteins in Table 1. (**B**) Immunoblot analyses of the same cellular fractions (5 μg of protein) with antibodies against caveolin-1 (caveolin) or insulin receptor β-subunit (IR).

proteins (Table 1). Immunoblot analysis also revealed the presence of nuclear histone H1 in this membrane fraction, but not in the caveolae fraction (results not shown).

Vectorial proteomics of caveolae

The isolation of caveolae should produce vesicles with an inside-orientated extracellular membrane surface in accord with the original shape of these membrane domains in adipocytes [3]. We subjected the caveolae vesicles to proteolytic treatment with trypsin and separated the remaining membrane proteins by gel electrophoresis. The difference in protein patterns before and after proteolysis demonstrated degradation of most of the caveolae proteins by trypsin (Figure 2A). However, two proteins with relative molecular masses of 70 and 100 kDa strongly resisted proteolysis in the caveolae vesicles (Figure 2A). Quantification of the relative amounts of each of these proteins before and after proteolysis in repetitive experiments showed only 20–30 % reduction in their amount after the trypsin treatment. The degradation of both proteins by trypsin was significantly increased after disruption of caveolae using the detergent Triton X-100 at 37 °C (results not shown). The results indicated that isolated caveolae conceal the 70 and 100 kDa proteins inside the vesicles.

The two proteins protected from proteolysis in the vesicles were excised after SDS/PAGE and subjected to in-gel digestion with trypsin. The generated peptides were analysed by MALDI–TOF-MS and peptide 'fingerprint' analysis, as well as by ESI–CID sequencing (Table 2). The 70 kDa protein was identified as CD36,

Table 1 Identification of proteins in the mitochondrial/nuclear fraction

Protein bands are numbered according to Figure 1(A). The superscript numbers correspond to the amino acid positions of the peptides in the sequences of corresponding proteins.

Band	Identified protein	NCBI accession no.	Calculated molecular mass (kDa)	Peptide sequences obtained by ESI and CID MS
1	Succinate dehydrogenase flavoprotein	1169337	73.7	A^{76}AFGLSEAGFNTACVTK^{92} E^{398}PIPVLPTVHYNMGGIPTNYK^{418}
2	Chaperonin HSP60	306890	61.1	L^{97}VQDVANNTNEEAGDGTTTATVLAR^{121} I^{251}SSIQSIVPALEIANAHR^{268} A^{430}AVEEGIVLGGGCALLR^{446}
3	Mitochondrial aldehyde dehydrogenase 2	25777732	56.9	L^{196}GPALATGNVVVMK^{209} V^{210}AEQTPLTALYVANLIK^{226} T^{325}FVQEDIYDEFVER^{338}
4	F_1-ATP synthase, β-subunit	32189394	56.5	L^{95}VLEVAQHLGESTVR^{109} V^{282}ALTGLTVAEYFR^{294} F^{311}TQAGSEVSALLGR^{324}
5	Core I protein	468935	53.3	A^{143}VELLGDIVQNCSLEDSQIEKER^{165} D^{181}VVFNYLHATAFQGTPLAQAVEGPSENVR^{209} N^{397}ALVSHLDGTTPVCEDIGR^{415}
6	Hydroxyacyl dehydrogenase, β-subunit	4504327	51.5	T^{62}PFLLSGTSYK^{72} E^{96}VVDYIIFGTVIQEVK^{111}
	Acetyl-CoA acyltransferase 2	5174429	42.5	T^{15}PFGAYGGLLK^{25} V^{46}SPETVDSVIMGNVLQSSSDAIYLAR^{71} T^{341}NVNGGAIALGHPLGGSGSR^{360}
	Citrate synthase	4758076	51.9	G^{77}LVYETSVLDPDEGIR^{92} I^{383}VPNVLLEQGK^{393}
	β-Actin	14250401	41.3	V^{89}APEEHPVLLTEAPLNPK^{106} L^{209}CYVALDFEQEMATAASSSSLEK^{231}
7	Acetyl-CoA acetyltransferase 1	86728	45.5	T^{50}PIGSFLGSLSLLPATK^{66} L^{67}GSIAIQGAIEK^{78} I^{312}VAFADAAVEPIDFPIAPVYAASMVLK^{338}

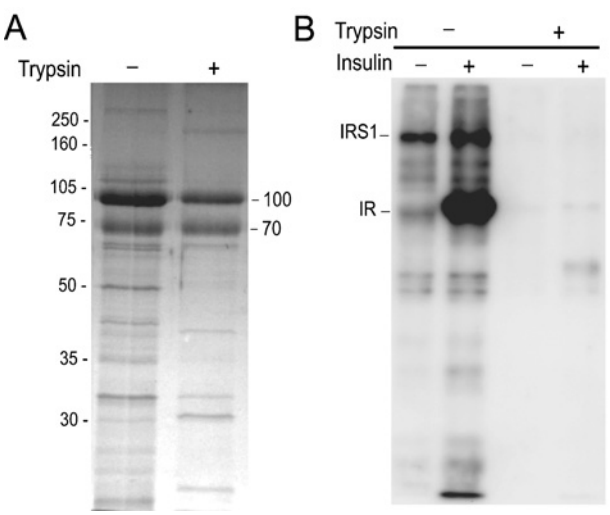

Figure 2 Proteolytic treatment of caveolae vesicles

(**A**) Protein pattern in isolated caveolae before and after treatment with trypsin, as indicated by − and + respectively (Coomassie Blue-stained gel; 8 μg of protein loaded). Positions of molecular-mass standards (kDa) are indicated. Two proteins that resisted tryptic treatment in caveolae are marked with their apparent molecular masses 100 and 70 kDa. (**B**) Immunoblot analysis of caveolae membrane proteins (3 μg of protein loaded) with antibodies against phosphotyrosine before and after treatment of the vesicles with trypsin, as indicated by − and + respectively. Caveolae were isolated from adipocytes that were stimulated with or without insulin, as indicated. Positions of insulin receptor (IR) and insulin receptor substrate 1 (IRS-1) are shown.

a transmembrane glycoprotein that has earlier been localized to caveolae in biochemical studies [24,25]. The membrane topology of CD36, in which only five N-terminal amino acids are exposed to the cytosol followed by a single transmembrane span and the rest of the protein is exposed to the extracellular space [26], explains the resistance to trypsin in caveolae vesicles. The 100 kDa protein was identified as a membrane copper-containing amine oxidase (Table 2). This protein is also referred to as semicarbazide-sensitive amine oxidase [27] or vascular adhesion protein VAP-1 in endothelial cells [28]. The membrane topology of this protein is similar to that of CD36, since it has a single N-terminal transmembrane span and the major part of the protein is exposed to the extracellular space [29]. The cell-surface-facing localization of this protein in caveolae of rat adipocytes has recently been confirmed by vectorial biotinylation and immunoblotting [14]. In addition to caveolin, CD36 and copper-containing amine oxidase were also determined as the major protein constituents of immunopurified caveolae from rat adipocytes [14].

Our results show that caveolae isolated in the absence of detergents form sealed vesicles, allowing vectorial analyses of the protein domains exposed to the opposite membrane sides. Accordingly, proteolytic treatment should cleave-off cytosol-exposed peptides of membrane proteins. To confirm this, we probed the susceptibility of tyrosine-phosphorylated cytosol-exposed protein domains to tryptic digestion. To this end, we isolated caveolae from adipocytes that were prestimulated with or without insulin (10 nM insulin at 37 °C for 15 min). Caveolae from both preparations were treated with trypsin and subjected to gel

Table 2 Identification of two caveolae-specific cell-surface-orientated proteins

The superscript numbers correspond to the amino acid positions of the peptides in the sequences of corresponding proteins. References to earlier caveolae localization of these proteins and determination of their membrane topology are presented.

Molecular mass (kDa)	Identified proteins	NCBI accession no.	MALDI–TOF No. of matched peptides at 30 p.p.m. (percentage sequence coverage)	Peptide sequences obtained by ESI and CID MS	Reference(s)
70	CD36	115982	11 (22)	S^{261}QVLQFFSSDICR^{273} T^{369}YLDIQPITGFTLQFAK^{385}	[24–26]
100	Copper-containing amine oxidase	4502119	12 (20)	L^{79}GPGLVDAAQAR^{90} E^{123}ALAIVFFGR^{132}	[14,28]

electrophoresis and immunoblotting with an antibody against phosphotyrosine. The level of tyrosine phosphorylation in caveolae from insulin-treated adipocytes was significantly increased and, more importantly, all the tyrosine-phosphorylated protein domains were removed from the vesicles by trypsin treatment (Figure 2B).

Caveolins are membrane-embedded polypeptides with their N- and C-termini exposed at the cytosolic surface, as reviewed in [1]. Owing to this membrane topology, caveolins were efficiently digested by trypsin in the isolated caveolae vesicles (Figure 3A). The mixture of peptides released from the surface of caveolae vesicles was analysed by nanospray-quadrupole-TOF MS. The resulting mass-to-charge spectrum (Figure 3B) showed that the peptide mixture was very complex, being a blend of fragments from proteins exposed on the caveolae surface. Detailed examination of such a mixture normally requires liquid chromatography preceding the MS analysis [30]. However, selection of the major ion species from the total peptide mixture in the mass filter of the mass spectrometer allowed a successful CID of these ions. CID spectra of peptide molecular ions with *m/z* 470.2, 599.8, 833.4 and 939.5 (Figure 3B) revealed sequences of tryptic peptides that originated from caveolin-1. This was consistent with caveolin being a major membrane protein component at the cytoplasmic surface of caveolae. The spectrum in Figure 3(C) shows the pattern of fragment ions produced by the molecular ion with *m/z* 470.2 (Figure 3B) and the identified sequence derived from caveolin-1 (amino acids 58–65). Using direct MS analysis of the caveolin peptides released from the surface of caveolae vesicles, we were able to identify for the first time the *in vivo* processing of caveolin-1α and -1β, which included excision of starting methionine residues and N-terminal acetylation [31]. Notably, earlier attempts of N-terminal microsequencing of caveolin-1α and -1β have failed because the N-termini of these proteins were found to be blocked [32]. Moreover, enrichment of phosphorylated peptides from the peptide mixture released from the surface of the caveolae vesicles and subsequent MS analyses allowed the identification of the phosphorylated residues Ser-5 and Ser-36 in mature caveolin-1β and -1α respectively [31]. Thus the specific morphology of isolated caveolae allows differential studies on membrane protein domains facing the extracellular space and the cytosol.

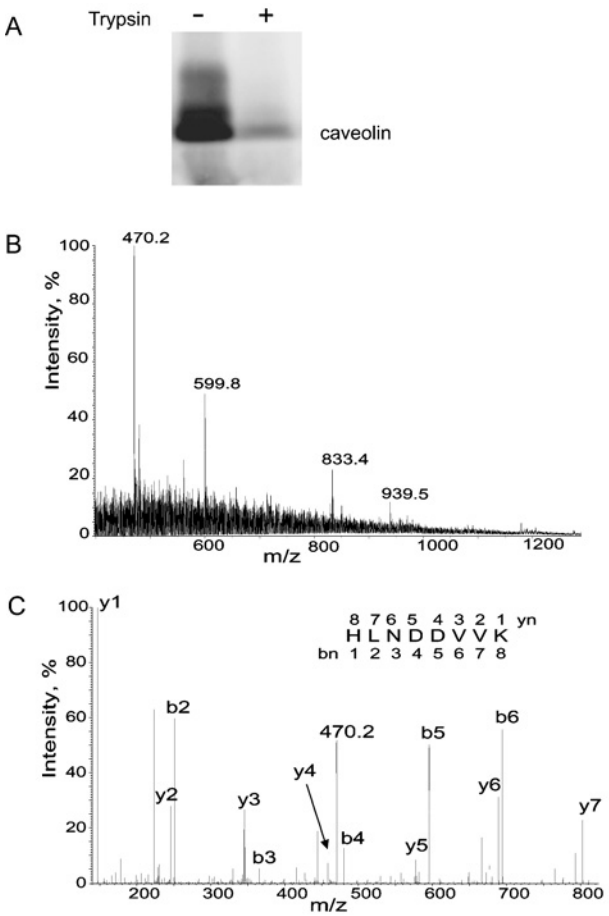

Figure 3 Analyses of caveolins exposed to the outer surface of caveolae vesicles

(**A**) Immunoblot analysis of caveolae proteins (3 μg of total protein loaded) with anti-caveolin-1 antibody before and after treatment of caveolae with trypsin, as indicated. (**B**) Full-scan ESI mass spectrum of the peptides released from the surface of caveolae vesicles by trypsin. (**C**) The product-ion spectrum of the doubly charged peptide ion with *m/z* 470.2 (also indicated in **B**) obtained by ESI and CID. The peptide fragment ions are represented as y (C-terminal) or b (N-terminal) fragments in the spectrum and are indicated in the shown peptide sequence obtained from the spectral data and corresponding to the sequence of caveolin-1.

Identification of peripheral proteins bound to the cytosolic surface of caveolae vesicles

To examine peripheral proteins bound at the cytoplasmic surface of caveolae from human adipocytes, we isolated caveolae after sonication of the isolated plasma membranes at mild ionic strength and pH. This was done to retain caveolae-associated peripheral proteins, which were then stripped from the vesicles by 0.5 M carbonate (pH 11) and separated from the membranes by centrifugation. Proteins from the pellet and supernatant were resolved by SDS/PAGE, which revealed specific enrichment of several polypeptides in the supernatant and demonstrated their peripheral localization at the cytoplasmic surface of caveolae (Figure 4). The protein pattern in the remaining caveolae membranes (Figure 4) was virtually identical with that in caveolae

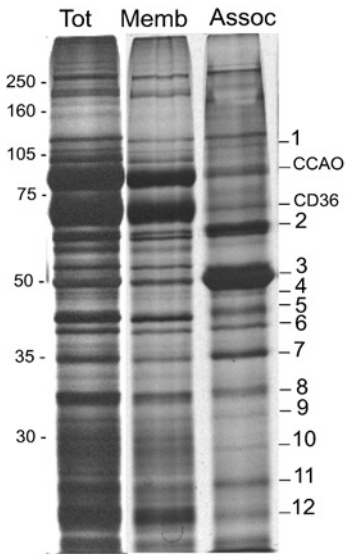

Figure 4 Identification of caveolae-associated proteins

Caveolae vesicles isolated at mild ionic strength and pH conditions were stripped of their associated proteins with 0.5 M carbonate buffer (pH 11). Aliquots containing 5 μg of caveolae proteins before treatment with the carbonate buffer (Tot), the remaining membrane proteins (Memb) and the released proteins (Assoc) were subjected to SDS/PAGE and silver staining. Positions of molecular-mass standards (kDa) are indicated. The numbers on the right correspond to the bands of caveolae-associated proteins that have been identified and described in the same order as in Table 3. CCAO, copper-containing amine oxidase.

isolated conventionally at pH 11 (Figure 1). The amount of peripheral proteins released from the vesicles isolated from different adipocyte preparations was always less than 10 % of the total caveolae protein, and the pattern of major caveolae-associated proteins (Figure 4) was very reproducible. Bands of caveolae-associated proteins were individually excised from the gel, digested with trypsin and subjected to peptide 'fingerprint' analyses and peptide sequencing by ESI and CID MS. A summary of the MS-based protein identification is presented in Table 3. Some of the excised protein bands contained several proteins. However, each one was identified by a combination of peptide mass 'fingerprinting' and sequencing of individual peptides from these proteins (Table 3).

Most of the peripheral proteins identified at the cytosolic surface of the caveolae vesicles (Table 3) have been shown recently to depend on cholesterol for their association with rafts in the plasma membrane of HeLa cells [18] and some have earlier been found in caveolae from different cell types [33–35] (see corresponding references in Table 3). However, six of the proteins, namely annexin V, R-Ras, Ras suppressor protein 1, SRBC (serum deprivation response-related gene product that binds to C-kinase; a protein kinase Cδ-binding protein), EHD2 (EHD-containing protein 2, where EHD stands for Eps15-homology domain) and PTRF, have not been specifically localized to caveolae previous to our work. Notably, PTRF was originally characterized as a transcription regulator [36]. The protein contains three leucine-zipper domains and two bipartite nuclear localization signals. The domain structure of PTRF is schematically represented in Figure 5, along with the structures of the caveolae-associated EHD2, SRBC and R-Ras, as well as the protein kinase Cα-binding protein called SDPR (serum deprivation response gene product; Table 3), which has earlier been found in caveolae of Rat-1 cells [37]. PTRF and EHD2 contain nuclear localization signal sequences (Figure 5). PTRF, SRBC and SDPR possess leucine-zipper domains and have homologous N-terminal regions [38,39]. A common feature of PTRF, EHD2, SRBC, SDPR and R-Ras is the presence of PEST domains in all five proteins (Figure 5). PEST sequences, being enriched in proline, glutamic acid, serine and threonine, serve as signals for the rapid proteolytic conversion of numerous signalling proteins [19]. Thus the finding of PEST domains in five proteins bound to the cytosolic surface of caveolae indicated a possible connection between their proteolytic regulation and targeting to caveolae.

Cellular distribution of PTRF

PTRF has initially been found as a nuclear factor required for the termination of transcription of rRNA in murine cells [36]. We found PTRF associated with caveolae in human adipocytes. This protein, designated as leucine-zipper protein FKSG13, has also been identified recently in lipid rafts in HeLa cells [18]. To establish the cellular distribution of PTRF, we probed the presence of this protein in the mitochondria/nuclear, cytosolic, microsomal, plasma-membrane and caveolae fractions of human adipocytes using a specific monoclonal antibody against the stretch of 116 amino acids in the central part of the PTRF sequence. PTRF was found to be highly enriched in plasma membrane and caveolae (Figure 6A). We made quantitative analyses of the immunoblots, which included all the cellular fractions and had been loaded with equal amounts of protein. Calculation of the amount of PTRF in these fractions, taking into account their volumes, established that 75–80 % of all PTRF in the fat cells was confined to the plasma membrane. In the plasma membranes, PTRF specifically associated with caveolae, as seen from immunoblotting of the fractions (Figure 6A). On the contrary, the relative amount of PTRF in the mitochondria/nuclear fraction was very low (Figure 6A). We also made separate dedicated preparations of nuclei [21] from the fat cells. Immunoblot analyses of the isolated nuclei and caveolae showed that the nuclear membrane protein, nucleoporin-p62, was largely depleted from the caveolae (Figure 6B), whereas the relative abundance of PTRF was much higher in the plasma membranes and caveolae than in the nuclei (Figure 6C). Nevertheless, PTRF was found in the nuclei by both immunoblotting (Figure 6C) and MS analysis (Table 4). MS analysis also revealed the abundance of nuclear histone H2B in the nuclear fraction (Table 4), but not in the caveolae fraction.

To ascertain the localization of PTRF at caveolae in the plasma membrane, we used immunofluorescence confocal microscopy. Plasma membranes from human adipocytes were labelled with fluorescent antibodies [3] against PTRF (Figure 7A) and caveolin (Figure 7B). Superimposition of the images (Figure 7C) clearly demonstrated co-localization of PTRF with caveolin at the cytosolic surface of the plasma membrane.

Proteolytic fragments of PTRF at the surface of caveolae

PTRF contains two PEST sequence modules, one in the middle of the protein and the other at the N-terminus (Figure 5). In agreement with the hypothesis of PEST sequences as proteolytic signals [19], we found a set of PTRF fragments in caveolae, corresponding to the apparent molecular masses of 47, 43, 30, 25 and 15 kDa (Figure 4 and Table 3). This pattern of truncated forms of PTRF bound to the surface of caveolae was highly reproducible between preparations and was not affected by the presence of a cocktail of protease inhibitors during the preparation of the plasma membranes and caveolae, which strongly indicated that proteolysis of PTRF occurred *in situ*, in the intact cells. Four of the PTRF fragments were also detected in the caveolae-associated proteins by immunoblotting against PTRF (Figure 6A). PTRF

Table 3 Identification of caveolae-associated proteins

The protein bands are numbered according to Figure 4. The superscript numbers correspond to the amino acid positions of peptides in the sequences of corresponding proteins. The last column gives references to earlier finding of the proteins in caveolae or lipid rafts.

Band	Identified proteins	NCBI accession no.	Calculated molecular mass (kDa)	MALDI–TOF sequence coverage at 50 p.p.m. (%)	Peptide sequences obtained by ESI and CID MS	Reference(s)
1	Myosin IC	24 415 400	118.0	29.0		[18,25]
2	EHD2	21 361 462	61.1	23.0	L^{33}LPLEEHYR^{41} G^{168}YDFPAVLR^{176} L^{270}FELEEQDLFR^{280} I^{342}QLEHHISPGDFPDCQK^{358}	
	Protein kinase Cα-binding protein (SDPR)	4 759 082	47.2		D^{49}NSQVNAVTVLTLLDK^{64} L^{65}VNMLDAVQENQHK^{78} V^{157}LIFQEENEIPASVFVK^{173}	[37]
	Annexin VI	113 962	75.9		S^{484}LEDALSSDTSGHFR^{498}	[17,18]
3	PTRF	28 395 016	43.5	12.0	M^{1}EDPTLYIVERPLPGYPDAEAPEP-SSAGAQAAEEPSGAGSEELIK^{45} S^{46}VQVNGVLVLSLLDK^{60} I^{61}IGAVDQIQLTQAQLEER^{78} Q^{79}AEMEGAVQSIQGELSK^{95} V^{153}MIYQDEVKLPAK^{165} E^{174}SEALPEKEGEELGEGERPEED-AAALELSSDEAVEVEEVLEESR^{217} K^{299}SFTPDHVVYAR^{310} V^{318}PPFTFHVK^{327} A^{338}TEMVEVGADDDEGGAER^{355}	
4	PTRF	28 395 016			S^{46}VQVNGVLVLSLLDK^{60} I^{61}IGAVDQIQLTQAQLEER^{78} Q^{79}AEMEGAVQSIQGELSK^{95}	
5	PTRF	28 395 016			S^{46}VQVNGVLVLSLLDK^{60} K^{137}LEVNEAELLR^{147} K^{299}SFTPDHVVYAR^{310}	
	α-Parvin	8 922 673	42.2		D^{118}LAEDLYDGQVLQK^{131}	
6	β-Actin	14 250 401	40.5	25.0		[17,18,25,33]
7	G_i-protein, α1-subunit	21 314 787	40.2	35.0	L^{91}KIDFGDSAR^{100} I^{162}AQPNYIPTQQDVLR^{176}	[18,25,34,35]
	G_i-protein, α2-subunit	4 504 041	40.3	37.0	A^{87}MGNLQIDFADPSR^{100} I^{163}AQSDYIPTQQDVLR^{177}	[18,25,34,35]
	G_s-protein, α-subunit				IEDYFPEFAR* QADYVPSDQDLLR*	[18,25,33–35]
	Protein kinase Cδ-binding protein (SRBC)	21 450 787	27.6	28.0	E^{3}SALEPGPVPEAPAGGPVHA-VTVVTLLEK^{31} L^{109}EANHGLLVAR^{119} E^{129}EGEVPASAFQK^{140}	[18]
8	Annexin II	18 645 167	38.6	28.0		[17,18,25,33]
9	Annexin V	17 391 477	35.9		M^{152}LVVLLQANR^{161} S^{246}IPAYLAETLYYAMK^{260}	
10	PTRF	28 395 016			S^{46}VQVNGVLVLSLLDK^{60}	
11	Ras suppressor protein 1	6 912 638	31.5		A^{138}LYLSDNDFEILPPDIGK^{155} L^{192}TVLPPELGNLDLTGQK^{208}	
	PTRF	28 395 016			S^{46}VQVNGVLVLSLLDK^{61}	[18]
12	R-Ras PTRF	5 454 028 28 395 016	23.5		L^{177}NVDEAFEQLVR^{188} S^{46}VQVNGVLVLSLLDK^{60} I^{61}GAVDQIQLTQAQLEER^{78}	

* These sequences match several G_s-protein α-subunit isoforms.

was one of the major proteins bound to the cytosolic surface of adipocyte caveolae (50 kDa band in Figure 4). MS analyses of the corresponding protein bands in the nuclear fraction (Table 4) and the cytosol fraction (results not shown) revealed the presence of PTRF in both the cellular compartments. However, the truncated forms of PTRF could not be detected in the nuclear or cytosol fractions.

MS characterization of the tryptic peptides from intact PTRF (50 kDa band in Figure 4) revealed two large peptides of 4710 and 4816 a.m.u. (1 a.m.u. = approx. 1.67×10^{-24} g). The comprehensive sequencing of such big polypeptides by tandem MS is rather unprecedented. However, using ESI quadrupole-TOF MS, we subjected the quadruply charged ions of both peptides to CID and obtained high-quality fragmentation spectra, which allowed

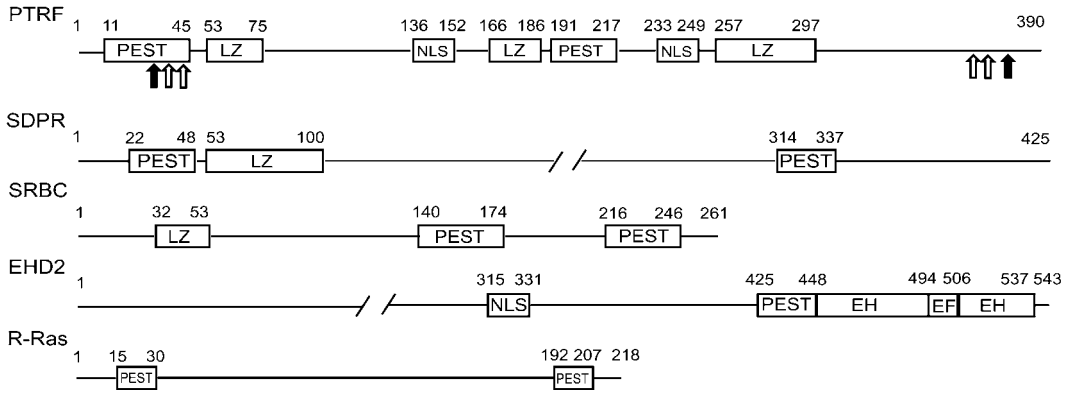

Figure 5 Structural similarities between five caveolae-associated proteins

Schematic representation of the domain structure of PTRF, SDPR, SRBC, EHD2 and R-Ras. Polypeptide modules are indicated as follows: LZ, leucine-zipper domain; PEST, PEST sequence; NLS, nuclear localization signal; EH, EHD; EF, calcium-binding motif. Numbers correspond to the first and last amino acids of the particular domain in the protein sequence. Solid and open arrows indicate non-tryptic cleavage sites and phosphorylated serine residues respectively in PTRF.

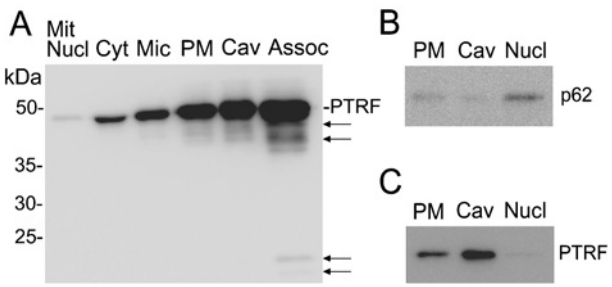

Figure 6 Distribution of PTRF in subcellular fractions

(**A**) Immunoblot analysis of mitochondrial/nuclear (Mit/Nucl), cytosol (Cyt), microsome (Mic), plasma-membrane (PM), caveolae (Cav) and caveolae-associated (Assoc) proteins (3 μg of protein loaded in each lane) with antibodies against PTRF. Positions of molecular-mass standards (kDa) are shown. Positions of PTRF fragments are indicated with arrows. (**B**) Immunoblot analysis of PM, Cav and Nucl proteins (2 μg of protein loaded) with antibodies against the nuclear membrane protein, nucleoporin-p62 (p62). (**C**) Immunoblot analysis of the same cellular fractions with antibodies against PTRF.

Table 4 Identification of PTRF and histone H2B in nuclear fraction isolated as described in [21]

The superscript numbers correspond to the amino acid positions of peptides in the PTRF sequence.

Identified protein	NCBI accession no.	Calculated molecular mass (kDa)	Peptide sequence obtained by ESI and CID MS
PTRF	28 395 016	43.5	S^{46}VQVNGVLVLSLLDK^{60} I^{61}IGAVDQIQLTQAQLEER^{78} K^{137}LEVNEAELLR^{147}
Histone H2B		14	LLLPGELAK* KESYSVYVYK* AMGIMNSFVNDIFER*

* These sequences match several histones of the H2B family.

reading of the complete 44- and 45-amino acid-long peptides comprising both the PEST sequences of PTRF (Table 3). Figure 8 demonstrates the fragmentation mass spectrum of the quadruply charged N-terminal peptide from PTRF with a comprehensive set of fragment ions. The overlapping ladders of b and y ions allowed reading of the entire 45-amino-acid-long sequence and revealed acetylation of the N-terminal methionine residue in this peptide (Figure 8). The peptide corresponds to the first 45 residues in the predicted sequence of human PTRF. We also found and sequenced the corresponding peptide with oxidized methionine (results not shown). In a similar way, we made a full *de novo* sequencing of a 44-amino-acid-long peptide, corresponding to residues 174–217 of PTRF and comprising the second PEST sequence (Table 3, spectrum not shown). Notably, we observed that CID of the quadruply charged peptide ions produced, in particular, the ions corresponding to the triply charged intact peptides (indicated by $M - 3H^{3+}$ in Figure 8 and results not shown). These ions were apparently generated by loss of one proton from the parent ion, which subsequently led to collision-induced fragmentation of both quadruply and triply charged peptide ions, yielding more comprehensive fragmentation patterns. The charge states of triply and doubly charged fragment ions (see Figure 8) were determined from their isotopic features revealed by the high resolution of the hybrid mass spectrometer. Thus, using ESI quadrupole-TOF MS for CID of quadruply charged ions allows sequencing of peptides longer than 40 amino acids.

Strikingly, the PEST sequence-containing peptides were detected in the intact PTRF, but not in any of the five truncated PTRF polypeptides found at the caveolae surface (Table 3). This finding suggests that the PEST sequence domains are the primary sites for proteolytic conversion of the caveolae-targeted PTRF.

Identification of four phosphorylation sites and two non-tryptic proteolytic cleavage sites in caveolae-associated PTRF

To probe for additional post-translational modifications of caveolae-associated proteins, we analysed them for the presence of phosphorylated peptides. The proteins released from the cytosolic surface of caveolae vesicles were digested with trypsin and phosphopeptides were then enriched by an IMAC procedure. The enriched phosphopeptides were subjected to ESI quadrupole-TOF MS analyses with CID. As a result, we identified four phosphorylated peptides, two of which were monophosphorylated and two were diphosphorylated. The CID fragmentation spectra of these peptides clearly demonstrated the presence of one or two phosphorylated residues in the corresponding peptides by the specific signals produced by neutral loss of one or two phosphoric acid molecules (Figures 9A and 9C and Figure 9B respectively). The spectra also revealed a couple of related peptides with the

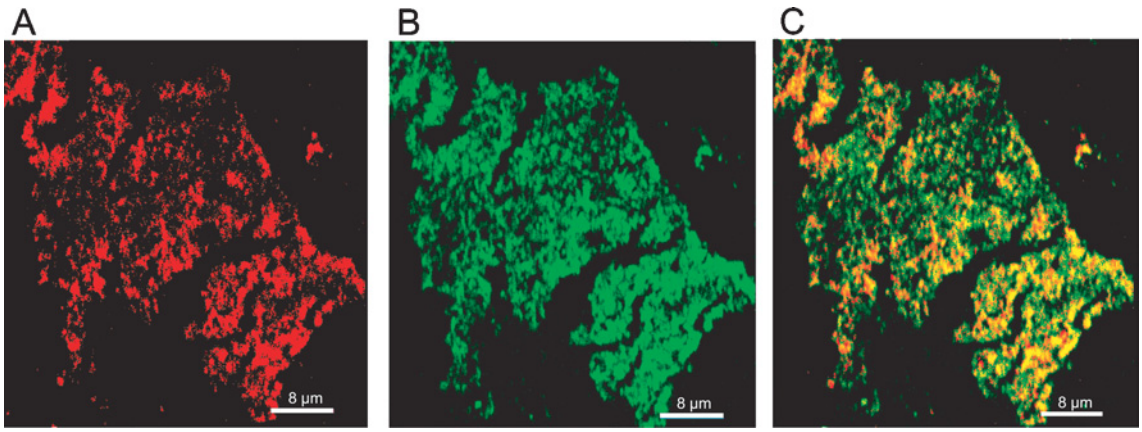

Figure 7 Co-localization of PTRF and caveolin in the plasma membrane of human adipocytes examined by immunofluorescence microscopy

The cytosolic surface of the plasma membrane was labelled with fluorescent antibodies against (**A**) PTRF (red) and (**B**) caveolin (green). (**C**) The superimposed images in (**A**) and (**B**) turn yellow where the red and green antibodies are co-localized.

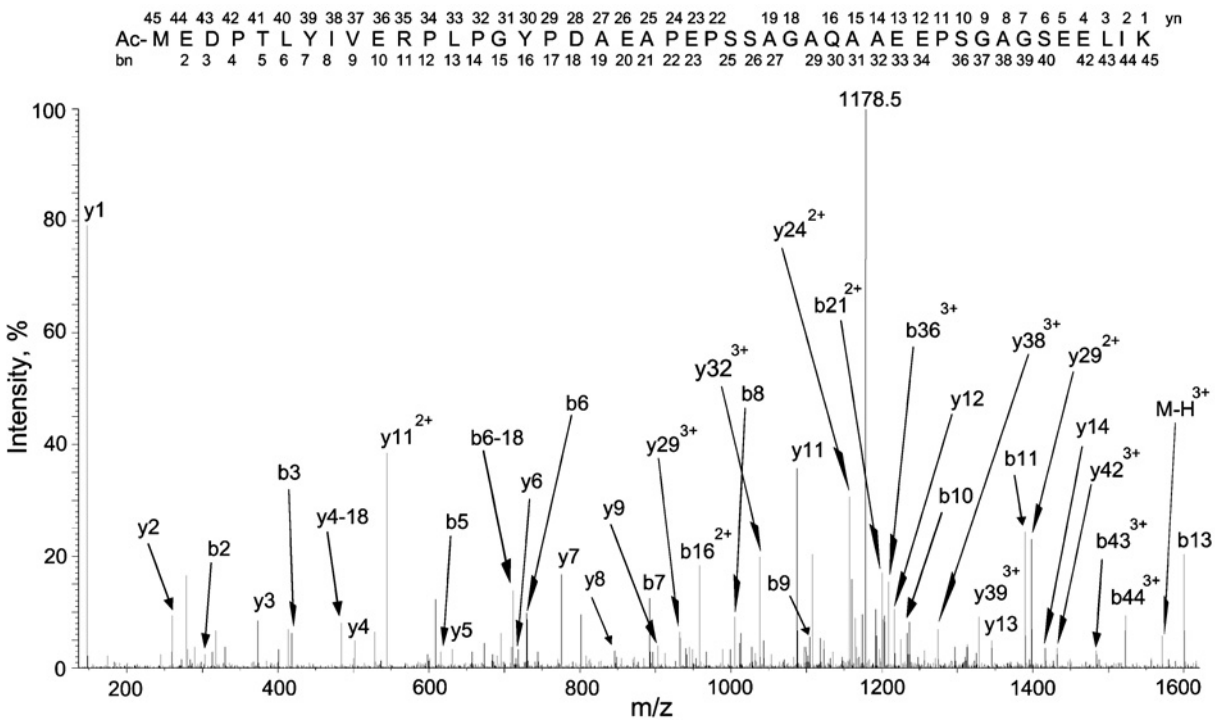

Figure 8 The ESI–CID product-ion spectrum revealing N-terminal acetylation and the PEST sequence of PTRF

The selected quadruply charged peptide ion with *m/z* 1178.5 (indicated) was subjected to CID. The fragment y (C-terminal) and b (N-terminal) ions having charge state higher than +1 are marked with the corresponding superscript numbers. The sequence of the acetylated 45-amino-acid-long peptide is shown with the numbered fragment ions that were identified in the spectrum.

same mono- and diphosphorylated peptide in each pair. MS sequencing uncovered the complete sequences and four distinct phosphorylation sites in the peptides (Figures 9A–9D), all of which corresponded to the PTRF sequence. One of the peptides originated from the C-terminal region of PTRF and comprised either phosphorylated Ser-365 or phosphorylated Ser-365 and the adjacent phosphorylated Ser-366 (Figures 9A and 9B). The other peptide matched the N-terminal PEST domain of PTRF and comprised either phosphorylated Ser-40 or phosphorylated Ser-36 and phosphorylated Ser-40 (Figures 9C and 9D). Each of the phosphorylated peptides contained one non-tryptic proteolytic cleavage site. In the C-terminal phosphopeptide, this cleavage site was between His-370 and Ala-371 in the PTRF sequence. The PEST sequences in the N-terminus of the protein had been cleaved between Gln-30 and Ala-31, which flanked the phosphorylated residues Ser-36 and Ser-40 in this domain of PTRF.

DISCUSSION

In the present study, we introduced the approach of vectorial proteomics to study protein topology in caveolae domains of

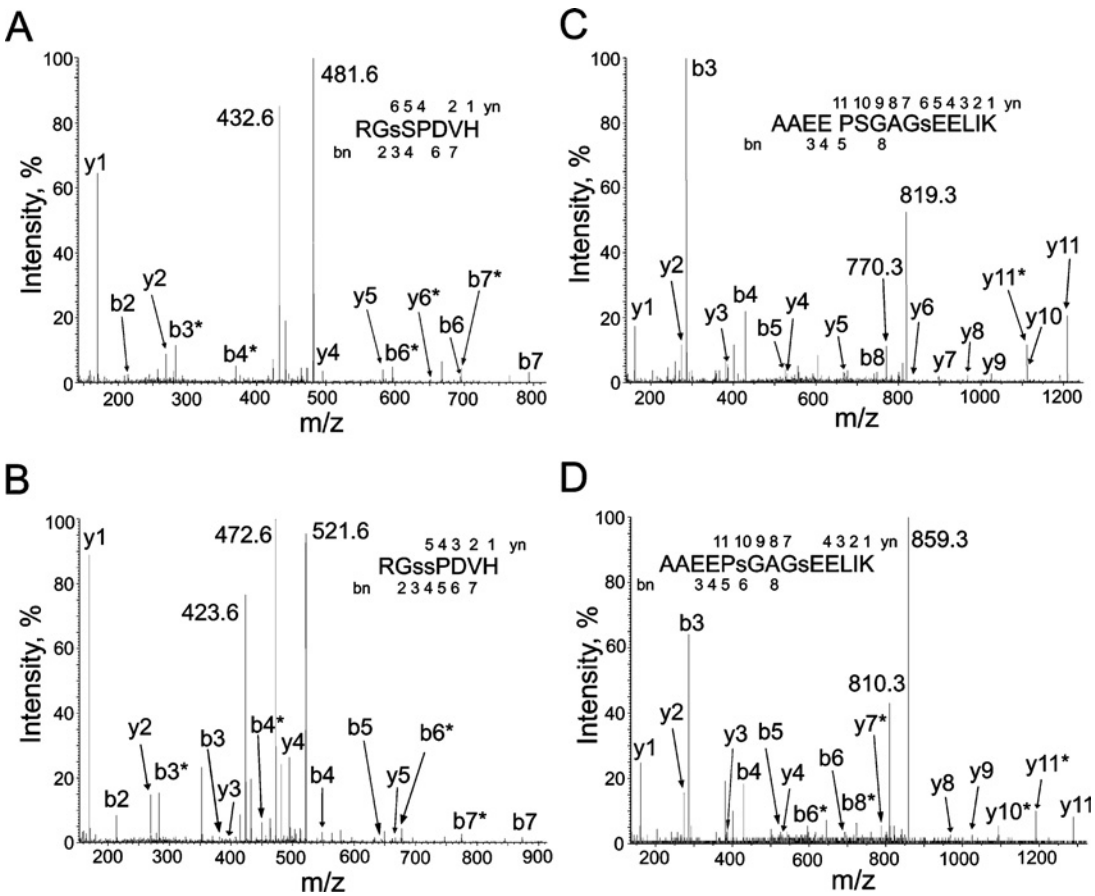

Figure 9 The ESI–CID product-ion spectra revealing non-tryptic cleavage sites and multiple phosphorylation of PTRF

The detected y (C-terminal) and b (N-terminal) ions are indicated in the spectra. The ions marked with asterisks indicate the fragments produced after neutral loss of H_3PO_4 (98 Da). (**A**) The doubly charged parent ion with *m/z* 481.6 is labelled in the spectrum along with the ion at *m/z* 432.6 produced after the neutral loss of 98 Da. The shown peptide sequence revealed from the spectrum corresponds to amino acids 363–370 in PTRF. The lower-case *s* indicates phosphorylation of Ser-365 in PTRF. (**B**) The doubly charged parent ion with *m/z* 521.6 is labelled in the spectrum along with the ions at *m/z* 472.6 and 423.6 produced after the single and double neutral losses of 98 Da respectively. The peptide sequence corresponds to amino acids 363–370 in PTRF, with phosphorylation of Ser-365 and Ser-366 indicated by the lower-case *s*. (**C**) The doubly charged parent ion with *m/z* 819.3 is labelled in the spectrum along with the ion at *m/z* 770.3 produced after the neutral loss of 98 Da. The peptide sequence corresponds to amino acids 31–45 in PTRF. The lower-case *s* indicates phosphorylation of Ser-40 in PTRF. (**D**) The parent ion with *m/z* 859.3 is labelled in the spectrum along with the ion at *m/z* 810.3 produced after the neutral loss of 98 Da. The peptide sequence corresponds to amino acids 31–45 in PTRF, with phosphorylation of Ser-36 and Ser-40 indicated by the lower-case *s*.

plasma membranes. This methodology exploits the property of caveolae to form sealed membrane vesicles after isolation in the absence of detergents and subsequent differential proteolytic treatments and MS analyses of the protein domains at the extracellular and cytosolic membrane surfaces. We applied this approach to study caveolae vesicles isolated from the physiologically relevant primary human adipocytes, whose plasma membranes are very high in caveolae [3]. The copper-containing amine oxidase and CD36 are shown to be the major extracellular-orientated proteins, whereas caveolin-1 is the main cytosol-orientated protein in these caveolae. Moreover, our method allowed the identification of peripheral proteins associated with the cytosolic face of caveolae, which revealed a protein context for the characterization of caveolae functions in human adipocytes.

The overview of the peripheral proteins identified at the cytosolic surface of caveolae (Table 3) allows us to group them broadly into two partly overlapping categories: first, proteins engaged in membrane–cytoskeleton interactions and, second, proteins participating in regulation and signal transduction. The structural proteins β-actin, α-parvin and myosin-IC (Table 3) could be involved in the dynamic interactions of caveolae with the cytoskeleton [2]. Annexins II, V and VI (Table 3) belong to a family of phospholipid- and actin-binding proteins that participate in the reversible formation of membrane–cytoskeleton complexes [40]. Annexins II and VI have been found in caveolae [40] and direct interaction of annexin II with caveolin has been demonstrated as well [41]. However, annexin V, a known inhibitor of phospholipase A and protein kinase C [42], has not been localized in caveolae previous to our work. EHD2 (Table 3), also found in caveolae for the first time, belongs to a family of conserved EHD-containing proteins [43], which function in endocytosis and in signal-transduction pathways downstream of receptor tyrosine kinases [44]. The association of EHD2 with human adipocyte caveolae may indicate that this isoform of the protein participates in caveolae vesicularization and endocytosis. EHD2 has a nuclear localization signal in its sequence (Figure 5) and can probably be relocated from caveolae to the nucleus or vice versa, similar to PTRF that is discussed below.

The protein kinase Cα-binding protein called SDPR (Table 3) has earlier been found in caveolae as a target of protein kinase Cα, which regulates membrane invagination [37]. Besides SDPR, we found that its homologue, the protein kinase Cδ-binding protein

SRBC [45], also bound to the surface of adipocyte caveolae (Table 3). This indicates that SRBC can function in the targeting of protein kinase Cδ to caveolae. SDPR and SRBC, as well as PTRF, contain leucine-zipper motifs (Figure 5) known as dimerization and protein–protein interaction modules [46]. All three proteins also have significant sequence homology in their N-terminal domains covering leucine zippers and stretching beyond them [39]. The leucine-zipper modules may determine protein involvement in the regulation of transcription [46]. Accordingly, SDPR and SRBC have been suggested to be involved in cell-cycle control [39] and PTRF has indeed been found to be a transcription regulator [36,47,48]. The fact that these proteins are found in caveolae of fat cells suggests the possible involvement of caveolae in cellular relocation of transcription regulators, particularly PTRF. In addition, it should be noted that caveolae are highly prevalent in the perinuclear region of adipocytes [3].

The mouse PTRF has been shown to be involved in termination of transcription by RNA polymerase I [36], hence in enhancement of this transcription [47] and in control of transcription by polymerase II [48]. Our results demonstrate that PTRF is a major protein associated with the cytosolic surface of caveolae in human fat cells. This finding is compatible with a recent unbiased proteomics study in HeLa cells, which determined PTRF as a component of lipid rafts [18]. Besides caveolae, we found PTRF in the other cellular membrane fractions, which probably also contained caveolae membranes, as well as in the cytosol. However, the relative amount of PTRF in the nuclei was surprisingly low, taking into account the function of this protein in regulation of transcription in the nucleus. Our findings also demonstrate that the amount of PTRF regulating transcription in the nucleus of fat cells is low and a large quantity of the protein is localized in the plasma membrane and caveolae. Moreover, using immunofluorescence confocal microscopy, we demonstrated co-localization of PTRF with caveolin at the cytosolic surface of plasma membranes. It is noteworthy that, in murine cells, PTRF has been found in transcriptionally active and inactive forms and displayed significant charge heterogeneity and phosphorylation at multiple sites, although phosphorylation sites have not been identified [47]. We found multiple forms of PTRF associated with caveolae vesicles, which include five proteolytic fragments of the protein and five post-translational modifications: N-terminal acetylation and four phosphorylation sites at distinct serine residues. We mapped the phosphorylation sites in PTRF to Ser-36, Ser-40, Ser-365 and Ser-366. The C-terminally located Ser-365 and Ser-366 are in the consensus sequences for phosphorylation by protein kinase A and casein kinase 2 respectively. Residues 363–368, comprising these phosphorylation sites, also constitute a class IV phosphorylation-dependent motif for interaction with WW-domain-containing proteins (where WW domain is a protein–protein interaction domain containing two conserved tryptophan residues) [49]. The N-terminal Ser-36 and Ser-40 constitute consensus sites for phosphorylation by glycogen synthase kinase-3. These two phosphorylated residues are localized in the PEST domain implicated in the proteolysis of PTRF. Thus it appears that the cytosolic surface of caveolae is the location of PTRF targeting, phosphorylation and proteolytic control.

PEST sequence is the usual signature for a protein to be targeted to proteolytic degradation [19]. In addition, the N-terminal amino acid of a protein and its acetylation is also a determinant of the lifespan of a protein [50]. In this respect, our finding of N-terminal acetylation of PTRF in the immediate vicinity of its first PEST sequence may indicate a critically controlled regulation of this protein through proteolytic conversion. Indeed, a significant fraction of PTRF in caveolae was identified as a reproducible set of protein fragments. Strikingly, neither of the two PEST sequence-containing peptides was detected in any of the caveolae-associated fragments of PTRF, whereas both peptides were found and completely sequenced from the full-length PTRF released from the caveolae vesicles. Our finding of two non-tryptic proteolytic cleavage sites, one of which is in the N-terminal PEST domain, suggests that they originate from the PTRF fragments bound to caveolae *in situ*. Importantly, both of the probably *in vivo* cleavage sites were flanked by phosphorylated serine residues. This indicates a possibility for phosphorylation-dependent fragmentation of PTRF at the cytosolic surface of caveolae membrane domains. Both the endogenous cleavage sites in PTRF satisfy sequential determinants for calpain-catalysed cleavage [51]. In agreement with this, calpain 5 has been found as an intrinsic component of lipid rafts in the membranes of HeLa cells [18]. Calpain cleavage sites are also known to occur preferentially within PEST domains [51]. These results point towards a high probability for such calpain-catalysed primary proteolytic cleavages within the PEST sequences of caveolae-bound PTRF. Caveolae-associated EHD2, SRBC, SDPR and R-Ras, all four of which also contain PEST sequences, could be regulated similarly. In conclusion, we propose an additional function for caveolae in adipocytes, which consists in targeting of PTRF and other PEST-domain-containing proteins and in controlling of their effective cellular concentrations by post-translational modifications and proteolysis.

We are grateful to H. Thorn (Division of Cell Biology, Linköping University) for expert assistance with confocal fluorescence microscopy. This work was supported by grants from the Swedish Research Council, Swedish Diabetes Association, Graduate Research School in Genomics and Bioinformatics (FGB) and Royal Swedish Academy of Sciences.

REFERENCES

1 Razani, B., Woodman, S. E. and Lisanti, M. P. (2002) Caveolae: from cell biology to animal physiology. Pharmacol. Rev. **54**, 431–467
2 van Deurs, B., Roepstorff, K., Hommelgaard, A. M. and Sandvig, K. (2003) Caveolae: anchored, multifunctional platforms in the lipid ocean. Trends Cell Biol. **13**, 92–100
3 Thorn, H., Stenkula, K. G., Karlsson, M., Örtegren, U., Nystrom, F. H., Gustavsson, J. and Strålfors, P. (2003) Cell surface orifices of caveolae and localization of caveolin to the necks of caveolae in adipocytes. Mol. Biol. Cell **14**, 3967–3976
4 Shaul, P. W. and Anderson, R. G. (1998) Role of plasmalemmal caveolae in signal transduction. Am. J. Physiol. **275**, 843–851
5 Smart, E. J., Graf, G. A., McNiven, M. A., Sessa, W. C., Engelman, J. A., Scherer, P. E., Okamoto, T. and Lisanti, M. P. (1999) Caveolins, liquid-ordered domains, and signal transduction. Mol. Cell. Biol. **19**, 7289–7304
6 Simons, K. and Toomre, D. (2000) Lipid rafts and signal transduction. Nat. Rev. Mol. Cell. Biol. **1**, 31–39
7 Gustavsson, J., Parpal, S., Karlsson, M., Ramsing, C., Thorn, H., Borg, M., Lindroth, M., Peterson, K. H., Magnusson, K. E. and Strålfors, P. (1999) Localization of the insulin receptor in caveolae of adipocyte plasma membrane. FASEB J. **13**, 1961–1971
8 Örtegren, U., Karlsson, M., Blazic, N., Blomqvist, M., Nystrom, F. H., Gustavsson, J., Fredman, P. and Strålfors, P. (2004) Lipids and glycosphingolipids in caveolae and surrounding plasma membrane of primary rat adipocytes. Eur. J. Biochem. **271**, 2028–2036
9 Fra, A. M., Williamson, E., Simons, K. and Parton, R. G. (1995) De novo formation of caveolae in lymphocytes by expression of VIP21-caveolin. Proc. Natl. Acad. Sci. U.S.A. **92**, 8655–8659
10 Williams, T. M. and Lisanti, M. P. (2004) The caveolin proteins. Genome Biol. **5**, 214
11 Stan, R. V., Roberts, W. G., Predescu, D., Ihida, K., Saucan, L., Ghitescu, L. and Palade, G. E. (1997) Immunoisolation and partial characterization of endothelial plasmalemmal vesicles (caveolae). Mol. Biol. Cell **8**, 595–605
12 Smart, E. J., Ying, Y. S., Mineo, C. and Anderson, R. G. (1995) A detergent-free method for purifying caveolae membrane from tissue culture cells. Proc. Natl. Acad. Sci. U.S.A. **92**, 10104–10108
13 Song, K. S., Li, S., Okamoto, T., Quilliam, L. A., Sargiacomo, M. and Lisanti, M. P. (1996) Co-purification and direct interaction of Ras with caveolin, an integral membrane protein of caveolae microdomains. Detergent-free purification of caveolae microdomains. J. Biol. Chem. **271**, 9690–9697

14 Souto, R. P., Vallega, G., Wharton, J., Vinten, J., Tranum-Jensen, J. and Pilch, P. F. (2003) Immunopurification and characterization of rat adipocyte caveolae suggest their dissociation from insulin signaling. J. Biol. Chem. **278**, 18321–18329
15 von Haller, P. D., Donohoe, S., Goodlett, D. R., Aebersold, R. and Watts, J. D. (2001) Mass spectrometric characterization of proteins extracted from Jurkat T cell detergent-resistant membrane domains. Proteomics **1**, 1010–1021
16 Bini, L., Pacini, S., Liberatori, S., Valensin, S., Pellegrini, M., Raggiaschi, R., Pallini, V. and Baldari, C. T. (2003) Extensive temporally regulated reorganization of the lipid raft proteome following T-cell antigen receptor triggering. Biochem. J. **369**, 301–309
17 Sprenger, R. R., Speijer, D., Back, J. W., De Koster, C. G., Pannekoek, H. and Horrevoets, A. J. (2004) Comparative proteomics of human endothelial cell caveolae and rafts using two-dimensional gel electrophoresis and mass spectrometry. Electrophoresis **25**, 156–172
18 Foster, L. J., De Hoog, C. L. and Mann, M. (2003) Unbiased quantitative proteomics of lipid rafts reveals high specificity for signaling factors. Proc. Natl. Acad. Sci. U.S.A. **100**, 5813–5818
19 Rechsteiner, M. and Rogers, S. W. (1996) PEST sequences and regulation by proteolysis. Trends Biochem. Sci. **21**, 267–271
20 Oka, Y. and Czech, M. P. (1984) Photoaffinity labeling of insulin-sensitive hexose transporters in intact rat adipocytes. Direct evidence that latent transporters become exposed to the extracellular space in response to insulin. J. Biol. Chem. **259**, 8125–8133
21 Kim, S. J. and Kahn, C. R. (1994) Insulin stimulates phosphorylation of c-Jun, c-Fos, and Fos-related proteins in cultured adipocytes. J. Biol. Chem. **269**, 11887–11892
22 Ficarro, S. B., McCleland, M. L., Stukenberg, P. T., Burke, D. J., Ross, M. M., Shabanowitz, J., Hunt, D. F. and White, F. M. (2002) Phosphoproteome analysis by mass spectrometry and its application to Saccharomyces cerevisiae. Nat. Biotechnol. **20**, 301–305
23 Shevchenko, A., Chernushevic, I., Wilm, M. and Mann, M. (2002) 'De novo' sequencing of peptides recovered from in-gel digested proteins by nanoelectrospray tandem mass spectrometry. Mol. Biotechnol. **20**, 107–118
24 Dorahy, D. J., Lincz, L. F., Meldrum, C. J. and Burns, G. F. (1996) Biochemical isolation of a membrane microdomain from resting platelets highly enriched in the plasma membrane glycoprotein CD36. Biochem. J. **319**, 67–72
25 Lisanti, M. P., Scherer, P. E., Vidugiriene, J., Tang, Z., Hermanowski-Vosatka, A., Tu, Y. H., Cook, R. F. and Sargiacomo, M. (1994) Characterization of caveolin-rich membrane domains isolated from an endothelial-rich source: implications for human disease. J. Cell Biol. **126**, 111–126
26 Tandon, N. N., Lipsky, R. H., Burgess, W. H. and Jamieson, G. A. (1989) Isolation and characterization of platelet glycoprotein IV (CD36). J. Biol. Chem. **264**, 7570–7575
27 Jalkanen, S. and Salmi, M. (2001) Cell surface monoamine oxidases: enzymes in search of a function. EMBO J. **20**, 3893–3901
28 Jaakkola, K., Kaunismaki, K., Tohka, S., Yegutkin, G., Vanttinen, E., Havia, T., Pelliniemi, L. J., Virolainen, M., Jalkanen, S. and Salmi, M. (1999) Human vascular adhesion protein-1 in smooth muscle cells. Am. J. Pathol. **155**, 1953–1965
29 Morris, N. J., Ducret, A., Aebersold, R., Ross, S. A., Keller, S. R. and Lienhard, G. E. (1997) Membrane amine oxidase cloning and identification as a major protein in the adipocyte plasma membrane. J. Biol. Chem. **272**, 9388–9392
30 Vener, A. V., Harms, A., Sussman, M. R. and Vierstra, R. D. (2001) Mass spectrometric resolution of reversible protein phosphorylation in photosynthetic membranes of Arabidopsis thaliana. J. Biol. Chem. **276**, 6959–6966
31 Vainonen, J. P., Aboulaich, N., Turkina, M. V., Strålfors, P. and Vener, A. V. (2004) N-terminal processing and modifications of caveolin-1 in caveolae from human adipocytes. Biochem. Biophys. Res. Commun. **320**, 480–486
32 Scherer, P. E., Tang, Z., Chun, M., Sargiacomo, M., Lodish, H. F. and Lisanti, M. P. (1995) Caveolin isoforms differ in their N-terminal protein sequence and subcellular distribution. Identification and epitope mapping of an isoform-specific monoclonal antibody probe. J. Biol. Chem. **270**, 16395–16401
33 Oh, P. and Schnitzer, J. E. (1999) Immunoisolation of caveolae with high affinity antibody binding to the oligomeric caveolin cage. Toward understanding the basis of purification. J. Biol. Chem. **274**, 23144–23154
34 Li, S., Couet, J. and Lisanti, M. P. (1996) Src tyrosine kinases, Galpha subunits, and H-Ras share a common membrane-anchored scaffolding protein, caveolin. Caveolin binding negatively regulates the auto-activation of Src tyrosine kinases. J. Biol. Chem. **271**, 29182–29190
35 Rybin, V. O., Xu, X., Lisanti, M. P. and Steinberg, S. F. (2000) Differential targeting of beta-adrenergic receptor subtypes and adenylyl cyclase to cardiomyocyte caveolae. A mechanism to functionally regulate the cAMP signaling pathway. J. Biol. Chem. **275**, 41447–41457
36 Jansa, P., Mason, S. W., Hoffmann-Rohrer, U. and Grummt, I. (1998) Cloning and functional characterization of PTRF, a novel protein which induces dissociation of paused ternary transcription complexes. EMBO J. **17**, 2855–2864
37 Mineo, C., Ying, Y. S., Chapline, C., Jaken, S. and Anderson, R. G. (1998) Targeting of protein kinase Calpha to caveolae. J. Cell Biol. **141**, 601–610
38 Gustincich, S., Vatta, P., Goruppi, S., Wolf, M., Saccone, S., Della Valle, G., Baggiolini, M. and Schneider, C. (1999) The human serum deprivation response gene (SDPR) maps to 2q32-q33 and codes for a phosphatidylserine-binding protein. Genomics **57**, 120–129
39 Xu, X. L., Wu, L. C., Du, F., Davis, A., Peyton, M., Tomizawa, Y., Maitra, A., Tomlinson, G., Gazdar, A. F., Weissman, B. E. et al. (2001) Inactivation of human SRBC, located within the 11p15.5–p15.4 tumor suppressor region, in breast and lung cancers. Cancer Res. **61**, 7943–7949
40 Babiychuk, E. B., Palstra, R. J., Schaller, J., Kampfer, U. and Draeger, A. (1999) Annexin VI participates in the formation of a reversible, membrane-cytoskeleton complex in smooth muscle cells. J. Biol. Chem. **274**, 35191–35195
41 Uittenbogaard, A., Everson, W. V., Matveev, S. V. and Smart, E. J. (2002) Cholesteryl ester is transported from caveolae to internal membranes as part of a caveolin-annexin II lipid-protein complex. J. Biol. Chem. **277**, 4925–4931
42 Russo-Marie, F. (1999) Annexin V and phospholipid metabolism. Clin. Chem. Lab. Med. **37**, 287–291
43 Pohl, U., Smith, J. S., Tachibana, I., Ueki, K., Lee, H. K., Ramaswamy, S., Wu, Q., Mohrenweiser, H. W., Jenkins, R. B. and Louis, D. N. (2000) EHD2, EHD3, and EHD4 encode novel members of a highly conserved family of EH domain-containing proteins. Genomics **63**, 255–262
44 Mayer, B. J. (1999) Endocytosis: EH domains lend a hand. Curr. Biol. **9**, 70–73
45 Izumi, Y., Hirai, S., Tamai, Y., Fujise-Matsuoka, A., Nishimura, Y. and Ohno, S. (1997) A protein kinase Cdelta-binding protein SRBC whose expression is induced by serum starvation. J. Biol. Chem. **272**, 7381–7389
46 Norton, J. D., Deed, R. W., Craggs, G. and Sablitzky, F. (1998) Id helix-loop-helix proteins in cell growth and differentiation. Trends Cell Biol. **8**, 58–65
47 Jansa, P., Burek, C., Sander, E. E. and Grummt, I. (2001) The transcript release factor PTRF augments ribosomal gene transcription by facilitating reinitiation of RNA polymerase I. Nucleic Acids Res. **29**, 423–429
48 Hasegawa, T., Takeuchi, A., Miyaishi, O., Xiao, H., Mao, J. and Isobe, K. (2000) PTRF (polymerase I and transcript-release factor) is tissue-specific and interacts with the BFCOL1 (binding factor of a type-I collagen promoter) zinc-finger transcription factor which binds to the two mouse type-I collagen gene promoters. Biochem. J. **347**, 55–59
49 Kato, Y., Ito, M., Kawai, K., Nagata, K. and Tanokura, M. (2002) Determinants of ligand specificity in groups I and IV WW domains as studied by surface plasmon resonance and model building. J. Biol. Chem. **277**, 10173–10177
50 Varshavsky, A. (1996) The N-end rule: functions, mysteries, uses. Proc. Natl. Acad. Sci. U.S.A. **93**, 12142–12149
51 Tompa, P., Buzder-Lantos, P., Tantos, A., Farkas, A., Szilagyi, A., Banoczi, Z., Hudecz, F. and Friedrich, P. (2004) On the sequential determinants of calpain cleavage. J. Biol. Chem. **279**, 20775–20785

Received 19 April 2004/2 July 2004; accepted 9 July 2004
Published as BJ Immediate Publication 9 July 2004, DOI 10.1042/BJ20040647